**Journal of Information Systems Engineering and Management**
2025, 10(32s)
e-ISSN: 2468-4376
https://www.jisem-journal.com/

**Research Article**

# Chemical Reactions and Radiation Impact on the Dufour and Heat Source's effects on Casson fluid flows over an Inclined Oscillation Plate

C. Manigandan[1], S. Senthamilselvi[1,*], S.Bhavani[2],V. Rekha[3]
[1]*Department of Mathematics, Vels Institute of Science, Technology & Advanced Studies, Chenna-600117, Tamil Nadu, India*
[*]*Corresponding Author Email: msselvi2305@gmail.com*
[2]*Department of Mathematics, Rajalakshmi Engineering College, Chennai-602105, India*
[3]*Department of Mathematics, Vel Tech Multi Tech Dr. Rangarajan Dr. Sakunthala Engineering College, Chennai-600062, Tamilnadu, India*

**ARTICLE INFO**

Received: 30 Dec 2024

Revised: 16 Feb 2025

Accepted: 25 Feb 2025

**ABSTRACT**

**Introduction**: This study presents an analytical investigation of unsteady free convective hydromagnetic boundary layers, with a focus on the effects of Dufour, heat radiation, and chemical reactions on the flow of Casson fluid over an inclined oscillating plate. The system is considered under uniform temperature and varying concentration conditions, interacting with a rotating porous medium. The governing equations are formulated and solved using the Laplace transform method. The numerical results are illustrated graphically, highlighting variations in temperature, velocity, and concentration for different parameter values. The study of Casson fluid dynamics has garnered significant attention due to its applications in biomedical engineering, polymer processing, and other industrial processes. Understanding the influence of heat and mass transfer parameters such as the Dufour number (Df), thermal radiation (R), and chemical reaction (K) on Casson fluid flow is crucial for optimizing thermal management in various engineering applications.

**Objectives**: The objective of this research is to analyze the behavior of Casson fluid under the combined effects of rotation and a porous medium, examining how these factors influence temperature distribution, velocity profiles, and concentration fields. By comparing Casson fluid to Newtonian fluid, this study also highlights its unique flow characteristics

**Methods**: Using the Laplace transform method, the analytical solutions for temperature, velocity, and concentration are obtained. The numerical computations provide insights into the physical significance of key governing parameters.

**Results**: The study reveals the following key findings
**Velocity Profiles:** The Casson fluid exhibits higher velocities compared to Newtonian fluid due to its inherent rheological properties. The velocity is enhanced with an increase in the Grashof number (Gr) and heat source intensity but decreases as the radiation parameter increases.
**Temperature Variation:** The temperature of the fluid decreases with increasing values of Grashof number (Gr), Dufour number (Df), thermal radiation parameter (R), and chemical reaction parameter (K). However, a stronger heat source leads to an increase in temperature.
**Concentration Effects:** The concentration profile decreases with increasing values of the chemical reaction parameter (K) and Schmidt number (Sc), indicating enhanced mass diffusion effects.
**Conclusions :** This research provides an in-depth analysis of the unsteady free convective hydromagnetic boundary layers of Casson fluid in a rotating porous medium. The study highlights how temperature, velocity, and concentration profiles are influenced by key parameters such as the Dufour number, thermal radiation, and chemical reaction effects. These findings contribute to a deeper understanding of Casson fluid behavior in various industrial and scientific applications

**Keywords:** Dufour Effect, Radiation, Chemical Reaction, Casson Fluid, Rotation, Porous Medium, Free Convection

## INTRODUCTION

Numerous disciplines, including electrical power generation, magnetohydrodynamics, and geophysics, use magnetohydrodynamic fluxes. For this reason, research on them, both theoretical and experimental, is crucial in engineering and technology. Heat transfer between various geometries imbedded in porous media has numerous applications in both science and practice. These include of nuclear reactor cooling, packed-bed catalytic reactors, geothermal reservoirs, porous solid drying, thermal insulation, enhanced oil recovery, and subterranean energy transfer. Numerical models of convection and associated radiation Radiative heat transfer research is currently heavily focused on processes. Convective heat transfer in porous media has received a lot of attention lately due to its numerous technological applications. The effects of MHD on a rapidly starting vertical infinite plate that underwent temperature changes due to a transverse magnetic field were examined by Soundalgekar et al. [1]. The radiative free convection movement of a visibly thin gray gas past an endless vertical plate was studied by Soundalgekar and Takhar [2]. The effects of radiation and chemical reactions on the flow of MHD Casson fluid via a vertical plate that oscillates in a porous media were investigated by Kataria et al. [3]. When Dufour and chemical reactions were occurring, Vijayaragavan et al. [4] attempted to determine a theoretical solution to the problem of heat and mass transfer in MHD Casson fluid flow across a sloped porous plate.

Kavitha et al. [5] investigated a parabolic flow that passed over a rotating isothermal plate with uniform mass diffusion and temperature during a chemical reaction. An MHD parabolic flow that traveled over an accelerating rotating isothermal plate was also examined by Selvaraj et al. [6]. The Soret and MHD effects of parabolic flow over a rapidly moving vertical plate were investigated by Nanadakumar et al. [7]. In addition, while temperature radiation and chemical reactions occurred, the plate was rotating. Jothi and Selvaraj [8] investigated the effects of the heat source on MHD and the radiation-absorbing fluid flowing across an increasing-higher plate surrounded by a porous medium. Lakshmikaanth et al. [9] state that whereas temperature decreases with increasing radiation (R), temperature increases with increasing heat source (Q). A team of researchers led by Maran [10] looked on thermal diffusion, or the movement of mass and heat across a vertical plate during a chemical process. Convection flow was not controlled by MHD. The Hall and magnetic effects on a stream passing a vertical plate moving at a parabolically high speed were examined in another work by Aruna et al. [11]. The mass was dispersing uniformly as thermal radiation, and the heat was changing. Radha et al. [12] examined the magnetohydrodynamic effects on Casson fluid flow via a parabolic accelerated vertical plate with thermal resistance when the flow is not steady. Muthucumaraswamy Rajamanickam et al.'s work [13–14] examined the effects of free convection on the magnetohydrodynamic flow of a vertical plate moving at a constant temperature during a chemical reaction. They examined how heat and mass transport, as well as Hall and rotational phenomena, affect magnetohydrodynamic flow over a vertically oriented plate undergoing exponential acceleration. R.B. Hetnarski demonstrates the use of an algorithm to determine the formulas for inverse Laplace transforms in [15, 16]. In a porous medium with increasing temperature, Subhrajit Sarma and Nazibuddin Ahmed [17] investigated and resolved the Dufour effect of non-steady MHD flow via a vertical plate. Prakash and Selvaraj [18] investigated the effects of heat and radiation on MHD and parabolic motion in Casson fluids flowing on a vertical plate via a rotating porous material. Using computers, Prabhakar et al. [19] investigated the effects of spinning, diffusion, and thermodynamics on the flow of a heat-generating MHD Casson fluid past a moving porous plate. The impacts of Soret and Dufour on MHD Casson Fluid Over a Vertical Plate in the Presence of Chemical Reaction and Radiation were recognized and rectified by Ananda Reddy and Janardhan [20]. Palani and Arutchelvi [21] talked about the effects of Soret and Dufour as well as how an MHD nanofluid passes past a tilted plate. The work by Kumar and Vempati [22, 23] investigated how magnetohydrodynamics (MHD) affected a vertical plate that was infinite and fired quickly.off in the presence of a horizontal magnetic field while the temperature varies. The effects of chemical reactions on flow past a fast-moving vertical plate with varying temperatures and mass diffusion in the presence of a magnetic field were examined by Muthucumaraswamy Rajamanickan et al. [24–25]. The effects of cross diffusion and heat production on the mixed convective MHD flow of Casson fluid through a porous media with non-linear thermal radiation were investigated by Patel and Harshad R. [26]. Bond stability, kinetic stability, energy-related variables, Gc-MS, and molecules in coumarin 3-(1-methly-2-imiadazolythio)-1-oxoethly were discussed by Dhanalakshmi et al. in their work [27]. Karthikeyan et al. [28–29] used MHD in one work to investigate the rotational consequences of parabolic flow across an isothermal vertical plate. The Soret and Dufour effects on unsteady MHD convection flow across an infinite vertical porous plate were investigated by Gayathri et al. [30]. Thermal and radiative effects on an unsteady MHD Casson fluid past a rotating porous media with variable mass diffusion are studied by Prakash et al. [31].In this work, we

examined the Dufour effects on Casson fluid flow past an accelerating inclined oscillating plate to a rotating porous fluid with constant mass diffusion and temperature

## MATHEMATICAL ANALYSIS

An infinite inclined oscillating plate built in a rotating system, where the Hall current with rotation is incorporated in the porous medium and the Dufour effect is also taken into consideration, is traversed by an unsteady free hydromagnetic natural convective flow with heat and mass transfer. The fluid is viscous, incompressible, electrically conductive, and optically thick. The coordinate model is chosen so that the $x' -$ axis points upward towards the plate and the $y' -$ axis is perpendicular to the plate.Along the $x' -$ axis, the fluid and plate rotate in accordance with the standardised angular velocity Ω. The fluid and plate are maintained at the constant temperature $\mathrm{T}'$ and initially rest at period along $t' \leq 0$. Additionally, the species concentration at $\mathrm{C}'_{\infty}$ must be consistently preserved on the plate's surface and at any location inside the fluid. Plate statistics are migrating to their own planes with $u' = u_0 coswt$ velocity. A uniform transverse magnetic field $B_0$ is implemented in a direction parallel to $y' -$ axis. The flow temperature and species concentration on the plate surface is upturned to the uniform temperature about $\mathrm{T}'_{\mathrm{w}}$ and uniform species concentration $\mathrm{C}'_{\mathrm{w}}$ and consequently retained. Then under usual Boussinesq's approximation for the unsteady parabolic starting motion is governed by the following equation.

$$\frac{\partial \mathrm{u}'}{\partial \mathrm{t}'} - 2\Omega'\mathrm{v}' = \vartheta\left(1+\frac{1}{\gamma}\right)\frac{\partial^2 \mathrm{u}'}{\partial \mathrm{y}'^2} + \mathrm{g}\beta_{\mathrm{T}'}(\mathrm{T}' - \mathrm{T}'_{\infty})\cos\alpha + \mathrm{g}\beta_{\mathrm{C}'}(\mathrm{C}' - \mathrm{C}'_{\infty})\cos\alpha - \frac{\vartheta \mathrm{u}'}{k_1'} \tag{1}$$

$$\frac{\partial \mathrm{v}'}{\partial \mathrm{t}'} + 2\Omega'\mathrm{u}' = \vartheta\frac{\partial^2 \mathrm{v}'}{\partial \mathrm{y}'^2} - \frac{\vartheta u'}{k_1'} \tag{2}$$

$$\frac{\partial \theta'}{\partial t'} = \frac{k}{\rho C_p}\frac{\partial^2 \theta'}{\partial y'^2} - \frac{1}{\rho C_p}\frac{\partial q_r'}{\partial y'} + \frac{Q_0}{\rho C_p}(\mathrm{T}' - \mathrm{T}'_{\infty})' + \frac{D_m K_T}{C_s C_p}\frac{\partial^2 C'}{\partial y'^2} \tag{3}$$

$$\frac{\partial \mathrm{C}'}{\partial \mathrm{t}'} = \frac{1}{S_c}\frac{\partial^2 \mathrm{C}'}{\partial \mathrm{y}'^2} - \mathrm{k}'(\mathrm{C}' - \mathrm{C}'_{\infty}) \tag{4}$$

Under the initial and boundary conditions listed below

$$\left.\begin{array}{c} \mathrm{u}' = 0, \mathrm{v}' = 0\,, \mathrm{T}' = \mathrm{T}'_{\infty},\ \mathrm{C}' = \mathrm{C}'_{\infty},\ \text{for all } \mathrm{z}' \geq 0\,, \mathrm{t}' \leq 0 \\ \mathrm{u}' = u_0 coswt,\quad \mathrm{T}' = \mathrm{T}'_{\infty} + (\mathrm{T}'_{\mathrm{w}} - \mathrm{T}'_{\infty})\frac{\mathrm{t}'}{t_0}, C' = (\mathrm{C}'_{\mathrm{w}} - \mathrm{C}'_{\infty})\frac{\mathrm{t}'}{t_0} \\ \mathrm{u}' \to 0,\quad \mathrm{T}' \to \mathrm{T}'_{\infty},\ \mathrm{C}' \to \mathrm{C}'_{\infty}\ \text{as}\ \mathrm{z}' \to \infty \text{ and } \mathrm{t}' \geq 0 \end{array}\right\} \tag{5}$$

As we have optically thick Casson fluid, we can use Rosseland approximation [26]

$$\frac{\partial q_r}{\partial z'} = -4a^*\sigma(T'^4_{\infty} - T'^4) \tag{6}$$

It is assumed that the temperature differences within the flow are sufficiently small such $T'^4$ They may be exPressed as a linear function of the temperature. This is accomplished by expanding $T'^4$ the Taylor series about $\mathrm{T}'_{\infty}$, and neglecting higher-order terms, thus

$$T'^4 \cong 4T'^3_{\infty}\,T' - 3T'^4_{\infty} \tag{7}$$

The consequent dimensionless aggregate is

$$U = \frac{u'}{U_0},\ V = \frac{v'}{U_0},\ t = \frac{t'}{t_0},\ y = \frac{y'}{U_0 t_0}, \gamma = \frac{\mu_B\sqrt{2\pi_c}}{P_y}$$

$$\theta = \frac{T'-T'_{\infty}}{T'_w - T'_{\infty}}, G_r = \frac{g\beta(T'_w - T'_{\infty})}{u_0}, C = \frac{C'-C'_{\infty}}{C'_w - C'_{\infty}}, G_C = \frac{g\beta(C'-C'_{\infty})}{C'_w - C'_{\infty}}\ ,\ Q = \frac{Q_0 v^2}{kU_0^2} \tag{8}$$

$$P_r = \frac{\mu C_p}{k}\ ,\ K = \frac{vk_1}{U_0^2},\ S_c = \frac{v}{D}\ ,\ R = \frac{16a^*\sigma T'^3_{\infty}}{kU_0^2}$$

Substituting values from Eq. (6) and Eq. (7) in Eq. (3) and in Eqs. (1)–(4) and dropping out the notation (for simplicity) we get the non-dimensional equations are

$$\frac{\partial U}{\partial t} = \left(1+\frac{1}{\gamma}\right)\frac{\partial^2 U}{\partial y^2} + 2\Omega\mathrm{v} - Gr\theta(cos\alpha) + GcC(cos\alpha) - \frac{U}{k_1} \tag{9}$$

$$\frac{\partial V}{\partial t} = \left(1+\frac{1}{\gamma}\right)\frac{\partial^2 V}{\partial y^2} - 2\Omega v + \frac{M^2(hU-V)}{(1+h^2)} - \frac{V}{k_1} \tag{10}$$

$$\frac{\partial \theta}{\partial t} = \frac{1}{P_r}\frac{\partial^2 \theta}{\partial y^2} - R\theta + Q\theta + Df\frac{\partial^2 C}{\partial z^2} \tag{11}$$

$$\frac{\partial C}{\partial t} = \frac{1}{S_c}\frac{\partial^2 C}{\partial y^2} - KC \tag{12}$$

To solve equations (9) and (10), use $q' = U + iV$ we get

$$\frac{\partial q'}{\partial t} = G_r\theta cos(\alpha) + G_C C\cos(\alpha) + \left(1+\frac{1}{\gamma}\right)\frac{\partial^2 q}{\partial y^2} - m^* q' \tag{13}$$

$$\frac{\partial \theta}{\partial t} = \frac{1}{P_r}\frac{\partial^2 \theta}{\partial y^2} - R\theta + Q\theta + Df\frac{\partial^2 C}{\partial y^2} \tag{14}$$

$$\frac{\partial C}{\partial t} = \frac{1}{S_c}\frac{\partial^2 C}{\partial y^2} - KC \tag{15}$$

Here $m^* = 2\Omega + \frac{1}{k_1}$

The corresponding initial and boundary conditions are

$$\left.\begin{array}{c} q' = 0, \theta = 0, C = 0 \; for \; all \; y \; and \; t \le 0 \\ q' = coswt, \theta = 1, C = t \;\; for \; all \; y, t \ge 0 \\ q' \to 0, \theta \to 0, C \to 0 \; as \; y \to \infty. \end{array}\right\} \tag{16}$$

## SOLUTIONS

The equations (13), (14), and (15) contain dimensionless administering conditions and corresponding beginning and limit conditions. These equations can be solved using Laplace transforms. After one last inverse transform, the following method is used to get

$$C = \begin{bmatrix} \frac{1}{2}\left[e^{-2\eta\sqrt{ScKt}}\, erfc\left(\eta\sqrt{Sc} - \sqrt{Kt}\right) + e^{2\eta\sqrt{ScKt}}\, erfc\left(\eta\sqrt{Sc} + \sqrt{Kt}\right)\right] \\ -\frac{\eta\sqrt{Sc}t}{2\sqrt{K}}\left[e^{-2\eta\sqrt{ScKt}}\, erfc\left(\eta\sqrt{Sc} - \sqrt{Kt}\right) - e^{2\eta\sqrt{ScKt}}\, erfc\left(\eta\sqrt{Sc} + \sqrt{Kt}\right)\right] \end{bmatrix} \tag{17}$$

$$\theta = \theta_1 + \frac{PrDfSc}{(Sc-Pr)}\left[\frac{a+K}{a^2}(-\theta_2 + \theta_3 + \theta_4 - \theta_5) + \frac{K}{a}(-\theta_6 + \theta_7)\right] \tag{18}$$

where

$$\theta_1 = \frac{1}{2}\begin{bmatrix} e^{-2\eta\sqrt{Pr(R-Q)t}}\, erfc\left(\eta\sqrt{Pr} - \sqrt{(R-Q)t}\right) \\ +e^{2\eta\sqrt{Pr(R-Q)t}}\, erfc\left(\eta\sqrt{Pr} + \sqrt{(R-Q)t}\right) \end{bmatrix}$$

$$\theta_2 = \begin{bmatrix} \frac{1}{2}\left[e^{-2\eta\sqrt{ScKt}}\, erfc\left(\eta\sqrt{Sc} - \sqrt{Kt}\right) + e^{2\eta\sqrt{ScKt}}\, erfc\left(\eta\sqrt{Sc} + \sqrt{Kt}\right)\right] \\ -\frac{\eta\sqrt{Sc}t}{2\sqrt{K}}\left[e^{-2\eta\sqrt{ScKt}}\, erfc\left(\eta\sqrt{Sc} - \sqrt{Kt}\right) - e^{2\eta\sqrt{ScKt}}\, erfc\left(\eta\sqrt{Sc} + \sqrt{Kt}\right)\right] \end{bmatrix}$$

$$\theta_3 = \begin{bmatrix} \frac{1}{2}\begin{bmatrix} e^{-2\eta\sqrt{Pr(R-Q)t}}\, erfc\left(\eta\sqrt{Pr} - \sqrt{(R-Q)t}\right) \\ +e^{2\eta\sqrt{Pr(R-Q)t}}\, erfc\left(\eta\sqrt{Pr} + \sqrt{(R-Q)t}\right) \end{bmatrix} \\ -\frac{\eta\sqrt{\mathrm{Pr}}t}{2\sqrt{(R-Q)}}\begin{bmatrix} e^{-2\eta\sqrt{Pr(R-Q)t}}\, erfc\left(\eta\sqrt{Pr} - \sqrt{(R-Q)t}\right) \\ -e^{2\eta\sqrt{Pr(R-Q)t}}\, erfc\eta\sqrt{Pr} + \sqrt{(R-Q)t} \end{bmatrix} \end{bmatrix}$$

$$\theta_4 = \frac{e^{at}}{2}\left[e^{-2\eta\sqrt{Sc(a+K)t}}\, erfc\left(\eta\sqrt{Sc} - \sqrt{(a+K)t}\right) + e^{2\eta\sqrt{Sc(a+K)t}}\, erfc\left(\eta\sqrt{Sc} + \sqrt{(a+K)t}\right)\right]$$

$$\theta_5 = \frac{e^{at}}{2}\begin{bmatrix} e^{-2\eta\sqrt{Pr(a+R-Q)t}}\, erfc\left(\eta\sqrt{Pr} - \sqrt{(a+R-Q)t}\right) \\ +e^{2\eta\sqrt{Pr(a+R-Q)t}}\, erfc\eta\sqrt{Pr} + \sqrt{(a+R-Q)t} \end{bmatrix}$$

$$\theta_6 = \frac{1}{2}\left[e^{-2\eta\sqrt{ScKt}}\, erfc\left(\eta\sqrt{Sc} - \sqrt{Kt}\right) + e^{2\eta\sqrt{ScKt}}\, erfc\left(\eta\sqrt{Sc} + \sqrt{Kt}\right)\right]$$

$$\theta_7 = \frac{1}{2}\begin{bmatrix} e^{-2\eta\sqrt{Pr(R-Q)t}}\, erfc\left(\eta\sqrt{Pr} - \sqrt{(R-Q)t}\right) \\ +e^{2\eta\sqrt{Pr(R-Q)t}}\, erfc\left(\eta\sqrt{Pr} + \sqrt{(R-Q)t}\right)\end{bmatrix}$$

$$q' = \left\{\begin{array}{c} f_1 + f_2 + \frac{Gr(cos\alpha)}{(a_1 Pr-1)b}[-f_3 + f_4] \\ + \frac{Gr(cos\alpha)}{(Pr-Sc)}\frac{(\mathrm{Pr}\, Df\, Sc)}{(a_1 Sc-1)}\begin{bmatrix}\left(\frac{k+a}{a^2c^2}\right)(f_5 + f_6 - f_7) + \left(\frac{k}{ac}\right)(f_8 - f_9) \\ +\left(\frac{a+k}{a^2(a-c)}\right)(f_{10} - f_{11})\end{bmatrix} \\ + \frac{Gr(cos\alpha)}{(Pr-Sc)}\frac{(\mathrm{Pr}\, Df\, Sc)}{(a_1 Pr-1)}\begin{bmatrix}\left(\frac{k+a}{a^2b^2}\right)(-f_{12} - f_{13} + f_{14}) + \left(\frac{k}{ab}\right)(-f_{15} + f_{16}) \\ +\left(\frac{a+k}{a^2(a-b)}\right)(-f_{17} + f_{18})\end{bmatrix} \\ + \frac{Gr(cos\alpha)}{(Pr-Sc)c^2}[-f_{19} - f_{20} + -f_{21}] \\ - \frac{Gr(cos\alpha)}{(a_1 Pr-1)b}[-f_{22} + f_{23}] \\ - \frac{Gr(cos\alpha)}{(Pr-Sc)}\frac{(\mathrm{Pr}\, Df\, Sc)}{(a_1 Sc-1)}\begin{bmatrix}\left(\frac{k+a}{a^2c^2}\right)(f_{24} + f_{25} - f_{26}) + \left(\frac{k}{ac}\right)(f_{27} - f_{28}) \\ -\left(\frac{a+k}{a^2(a-c)}\right)(f_{29} - f_{30})\end{bmatrix} \\ - \frac{Gr(cos\alpha)}{(Pr-Sc)}\frac{(\mathrm{Pr}\, Df\, Sc)}{(a_1 Pr-1)}\begin{bmatrix}\left(\frac{k+a}{a^2b^2}\right)(-f_{31} - f_{32} + f_{33}) + \left(\frac{k}{ac}\right)(-f_{34} + f_{35}) \\ -\left(\frac{a+k}{a^2(a-b)}\right)(-f_{36} + f_{37})\end{bmatrix} \\ - \frac{Gr(cos\alpha)}{(a_1 Sc-1)c^2}[-f_{38} - f_{39}] \end{array}\right\} \tag{19}$$

$$f_{1=}\frac{e^{-iwt}}{4}\begin{bmatrix} e^{2\eta\sqrt{\frac{(m-iw)t}{a_1}}}\, erfc\left(\frac{\eta}{\sqrt{a_1}} + \sqrt{(m-iw)t}\right) \\ +e^{-2\eta\sqrt{\frac{(m-iw)t}{a_1}}}\, a_1 erfc\left(\frac{\eta}{\sqrt{a_1}} - \sqrt{(m-iw)t}\right)\end{bmatrix}$$

$$f_2 = \frac{e^{iwt}}{4}\begin{bmatrix} e^{2\eta\sqrt{\frac{(m+iw)t}{a_1}}}\, erfc\left(\frac{\eta}{\sqrt{a_1}} + \sqrt{(m+iw)t}\right) \\ +e^{-2\eta\sqrt{\frac{(m-iw)t}{a_1}}}\, erfc\left(\frac{\eta}{\sqrt{a_1}} - \sqrt{(m+iw)t}\right)\end{bmatrix}$$

$$f_3 = f_5 = f_8 = f_{12} = f_{15} = f_{19} = \frac{1}{2}\left[e^{-2\eta\sqrt{\frac{mt}{a_1}}} erfc\left(\eta - \sqrt{\frac{mt}{a_1}}\right) + e^{2\eta\sqrt{\frac{mt}{a_1}}} erfc\left(\eta + \sqrt{\frac{mt}{a_1}}\right)\right]$$

$$f_4 = \frac{e^{bt}}{2}\left[e^{-2\eta\sqrt{\frac{(m+b)t}{a_1}}} erfc\left(\eta - \sqrt{\frac{(m+b)t}{a_1}}\right) + e^{2\eta\sqrt{\frac{(m+b)t}{a_1}}} erfc\left(\eta + \sqrt{\frac{(m+b)t}{a_1}}\right)\right]$$

$$f_{20} = \begin{bmatrix} \frac{1}{2}\left(e^{2\eta\sqrt{\frac{mt}{a_1}}} erfc\left(\eta + \sqrt{\frac{mt}{a_1}}\right) + e^{-2\eta\sqrt{\frac{mt}{a_1}}} erfc\left(\eta - \sqrt{\frac{mt}{a_1}}\right)\right) \\ -\frac{\eta\sqrt{a_1}t}{2\sqrt{m}}\left[e^{-2\eta\sqrt{\frac{mt}{a_1}}}\, erfc\left(\eta - \sqrt{\frac{mt}{a_1}}\right) - e^{2\eta\sqrt{\frac{mt}{a_1}}}\, erfc\left(\eta + \sqrt{\frac{mt}{a_1}}\right)\right]\end{bmatrix}$$

$$f_7 = f_9 = f_{11} = \frac{e^{ct}}{2}\left[e^{-2\eta\sqrt{\frac{(m+c_1)t}{a_1}}} erfc\left(\eta - \sqrt{\frac{(m+c_1)t}{a_1}}\right) + e^{2\eta\sqrt{\frac{(m+c_1)t}{a_1}}} erfc\left(\eta + \sqrt{\frac{(m+c_1)t}{a_1}}\right)\right]$$

$$f_{10} = f_{17} = \frac{e^{at}}{2}\left[e^{-2\eta\sqrt{\frac{(m+a)t}{a_1}}}erfc\left(\eta - \sqrt{\frac{(m+a)t}{a_1}}\right) + e^{2\eta\sqrt{\frac{(m+a)t}{a_1}}}erfc\left(\eta + \sqrt{\frac{(m+a)t}{a_1}}\right)\right]$$

$$f_{14} = f_{16} = f_{18} = \frac{e^{bt}}{2}\left[e^{-2\eta\sqrt{\frac{(m+b)t}{a_1}}}erfc\left(\eta - \sqrt{\frac{(m+b)t}{a_1}}\right) + e^{2\eta\sqrt{\frac{(m+b)t}{a_1}}}erfc\left(\eta + \sqrt{\frac{(m+b)t}{a_1}}\right)\right]$$

$$f_{21} = \frac{e^{ct}}{2}\left[e^{-2\eta\sqrt{\frac{(m)t}{a_1}}}erfc\left(\eta - \sqrt{\frac{(m)t}{a_1}}\right) + e^{2\eta\sqrt{\frac{(m)t}{a_1}}}erfc\left(\eta + \sqrt{\frac{(m)t}{a_1}}\right)\right]$$

$$f_{22} = f_{31} == f_{34} = \frac{1}{2}\begin{bmatrix} e^{-2\eta\sqrt{Pr(R-Q)t}}erfc\left(\eta\sqrt{Pr} - \sqrt{(R-Q)t}\right) \\ +e^{2\eta\sqrt{Pr(R-Q)t}}erfc\left(\eta\sqrt{Pr} + \sqrt{(R-Q)t}\right)\end{bmatrix}$$

$$f_{23} = f_{37} = \frac{e^{bt}}{2}\begin{bmatrix} e^{-2\eta\sqrt{Pr(R+b-Q)t}}erfc\left(\eta\sqrt{Pr} - \sqrt{(R+b-Q)t}\right) \\ +e^{2\eta\sqrt{Pr(R+b-Q)t}}erfc\left(\eta\sqrt{Pr} + \sqrt{(R+b-Q)t}\right)\end{bmatrix}$$

$$f_{24} = f_{27} = f_{38} = \frac{1}{2}\left[e^{-2\eta\sqrt{Sckt}}erfc\left(\eta\sqrt{Sc} - \sqrt{kt}\right) + e^{2\eta\sqrt{Sckt}}erfc\left(\eta\sqrt{Sc} + \sqrt{kt}\right)\right]$$

$$f_{25} = f_{39} = \begin{bmatrix} \frac{1}{2}\left(e^{-2\eta\sqrt{Sckt}}erfc\left(\eta\sqrt{Sc} - \sqrt{kt}\right) + e^{2\eta\sqrt{Sckt}}erfc\left(\eta\sqrt{Sc} + \sqrt{kt}\right)\right) \\ -\frac{\eta\sqrt{Sc}t}{2\sqrt{K}}\left[e^{-2\eta\sqrt{Sckt}}erfc\left(\eta\sqrt{Sc} - \sqrt{kt}\right) + e^{2\eta\sqrt{Sckt}}erfc\left(\eta\sqrt{Sc} + \sqrt{kt}\right)\right]\end{bmatrix}$$

$$f_{26} = \frac{e^{ct}}{2}\begin{bmatrix} e^{-2\eta\sqrt{Sc(S+k)t}}erfc\left(\eta\sqrt{Sc} - \sqrt{(S+k)t}\right) \\ +e^{2\eta\sqrt{Sc(S+k)t}}erfc\left(\eta\sqrt{Sc} + \sqrt{(S+k)t}\right)\end{bmatrix}$$

$$f_{28=}\frac{e^{ct}}{2}\left(e^{-2\eta\sqrt{Sckt}}erfc\left(\eta\sqrt{Sc} - \sqrt{kt}\right) + e^{2\eta\sqrt{Sckt}}erfc\left(\eta\sqrt{Sc} + \sqrt{kt}\right)\right)$$

$$f_{29} = \frac{e^{at}}{2}\begin{bmatrix} e^{-2\eta\sqrt{Sc(a+k)t}}erfc\left(\eta\sqrt{Sc} - \sqrt{(a+k)t}\right) \\ +e^{2\eta\sqrt{Sc(a+k)t}}erfc\left(\eta\sqrt{Sc} + \sqrt{(a+k)t}\right)\end{bmatrix}$$

$$f_{30} = \frac{e^{ct}}{2}\begin{bmatrix} e^{-2\eta\sqrt{Sc(c+k)t}}erfc\left(\eta\sqrt{Sc} - \sqrt{(c+k)t}\right) \\ +e^{2\eta\sqrt{Sc(c+k)t}}erfc\left(\eta\sqrt{Sc} + \sqrt{(c+k)t}\right)\end{bmatrix}$$

$$f_{32} = b\begin{bmatrix} \frac{1}{2}\begin{pmatrix} e^{-2\eta\sqrt{Pr(R-Q)t}}erfc\left(\eta\sqrt{Pr} - \sqrt{(R-Q)t}\right) \\ +e^{2\eta\sqrt{Pr(R-Q)t}}erfc\left(\eta\sqrt{Pr} + \sqrt{(R-Q)t}\right)\end{pmatrix} \\ -\frac{\eta\sqrt{Pr}t}{2\sqrt{R-Q}}\left[\begin{pmatrix} e^{-2\eta\sqrt{Pr(R-Q)t}}erfc\left(\eta\sqrt{Pr} - \sqrt{(R-Q)t}\right) \\ -e^{2\eta\sqrt{Pr(R-Q)t}}erfc\left(\eta\sqrt{Pr} + \sqrt{(R-Q)t}\right)\end{pmatrix}\right]\end{bmatrix}$$

$$f_{33} = f_{35} = \frac{e^{bt}}{2}\begin{bmatrix} e^{-2\eta\sqrt{Pr(R+b-Q)t}}erfc\left(\eta\sqrt{Pr} - \sqrt{(R+b-Q)t}\right) \\ +e^{2\eta\sqrt{Pr(R+b-Q)t}}erfc\left(\eta\sqrt{Pr} + \sqrt{(R+b-Q)t}\right)\end{bmatrix}$$

$$f_{36} = \frac{e^{at}}{2}\left[\begin{matrix} e^{-2\eta\sqrt{Pr(R+a-Q)t}}erfc\left(\eta\sqrt{Pr} - \sqrt{(R+a-Q)t}\right) \\ +e^{2\eta\sqrt{Pr(R+a-Q)t}}erfc\left(\eta\sqrt{Pr} + \sqrt{(R+a-Q)t}\right)\end{matrix}\right]$$

$$erfc(a+ib) = \text{erf}(a) + \frac{\exp(-a^2)}{2a\pi}[1-\cos(2ab) + isin(2ab)]$$

$$+\frac{2\exp(-a^2)}{\pi}\sum_{n=1}^{\infty}\frac{\exp(-\eta^2/4)}{\eta^2+4a^2}[f_n(a,b) + ig_n(a,b)] + \in (a,b)$$

$$f_n = 2a - 2\,\text{acosh}(nb)\cos(2ab) + nsinh(nb)\sin(2ab) \quad \text{and}$$
$$g_n = 2\,\text{acosh}(nb)\sin(2ab) + nsinh(nb)\cos(2ab)$$

$$|\epsilon(a,b)| \approx\approx 10^{-16}|erf(a+ib)|$$

## RESULTS AND DISCUSSIONS

We are going to look at some numbers that show how different non-dimensional flow parameters affect the speed (q'), temperature (θ), and concentration (C) as they are plotted against the boundary layer coordinate ($\eta$) in Figures 2 through 20. These numbers include magnetic parameter (M), chemical reaction parameter (K), rotation parameter (R), Schmidt number (Sc), Grashof number (Gr), permeability parameter (k1), heat absorption coefficient (Q), Dufour number (Df), Casson fluid parameter ($\gamma$), and time t.

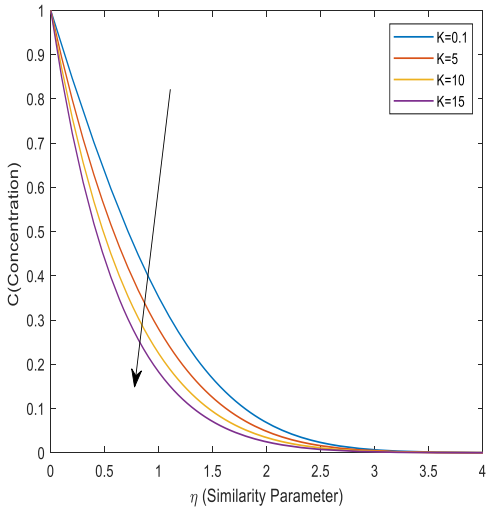


**Fig. 1.** Concentration curves observed for distinct values of K

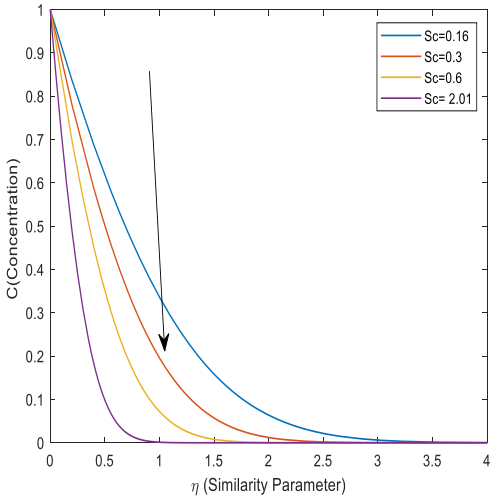


**Fig. 2.** Concentration curves Curves for distinguished Sc

Fig.1 illustrates the concentration goes to down as increase the chemical reaction values and using various Schmidt numbers, the result is seen in fig.2 when the Schmidt value is assumed to be high it may be noticed that the divided concentration rises.

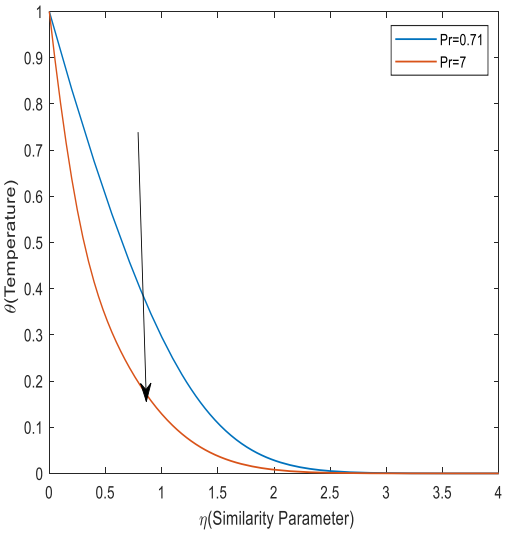


**Fig. 3.** Temperature Profiles for several values of Pr

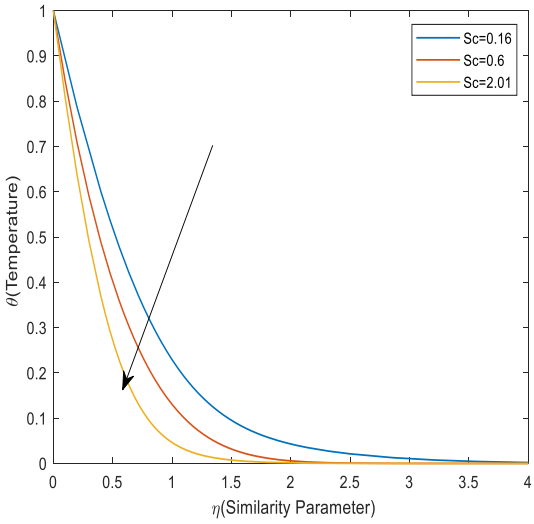


**Fig. 4.** Temperature Profiles for distinguished Sc values

In fig.3 shows that temperature decreases as in the values of Pr values increases and fig.4,it is observed that Schmidt number increases, indicating a tendency for the temperature to rise initially. However, the temperature subsequently fluctuates, revealing a change in trend, decrease in warm at this stage.

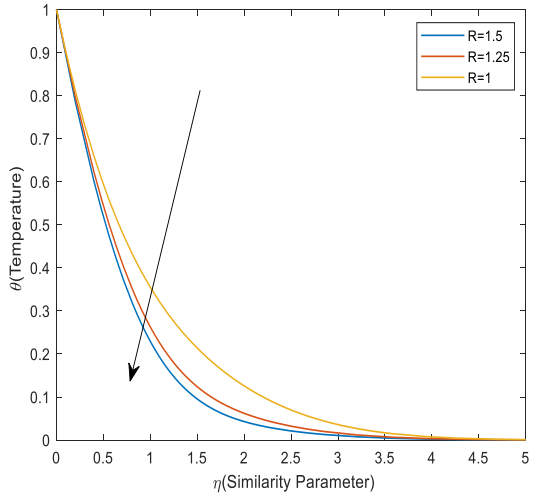


**Fig. 5.** Temperature Profiles for distinct values of R

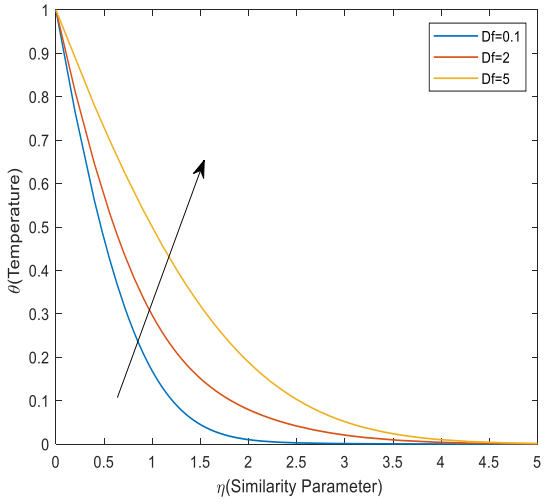


**Fig. 6.** Temperature Profiles for distinguished Df values

Fig. 5 illustrates the temperature Profile shows that Thermal radiation parameter R goes up, the temperature goes down and in fig.6, we can explore the heat behaviour in more detailed by considering the thermal diffusion(Dufour) numbers (Df = 0.1,1,2). In general, as Dufour parameter increases, it means that the Dufour effect becomes more Pronounced, and the temperature distribution within the mixture becomes more affected by the concentration gradients. This can lead to higher or lower temperatures depending on the specific circumstances and the sign of the Dufour effect

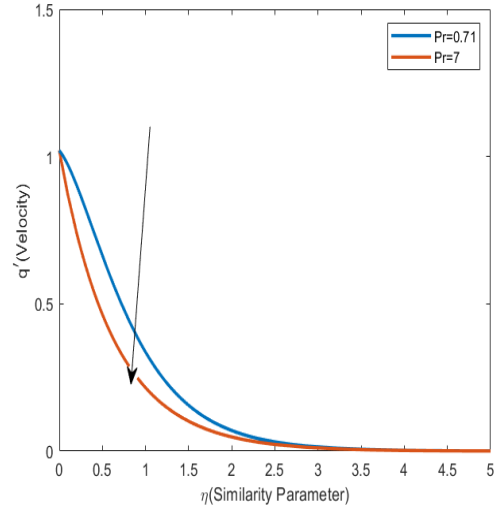


**Fig. 7.** Velocity Profile for different values of Pr

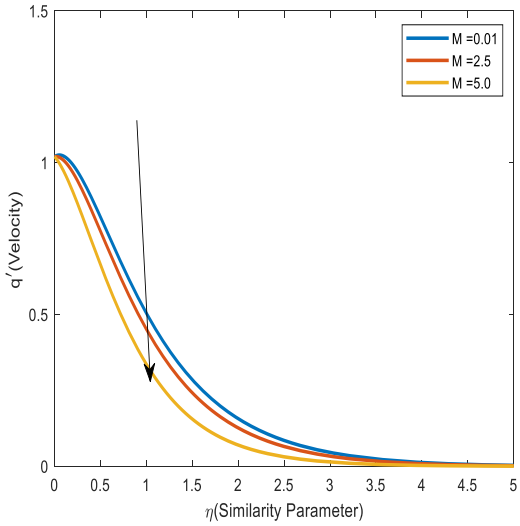


**Fig. 8.** Velocity Profile for different values of M

In fig.7 it is observed that velocity increases with increasing in the values of Prandtl number. In fig.8 it is considered that the influence of a magnetic field on fluid motion is measured using Hartmann values, which specifically gauge the reduction of velocity variations due to the magnetic field's Lorentz force. However, these values do not directly dictate the speed or orientation of the velocity.

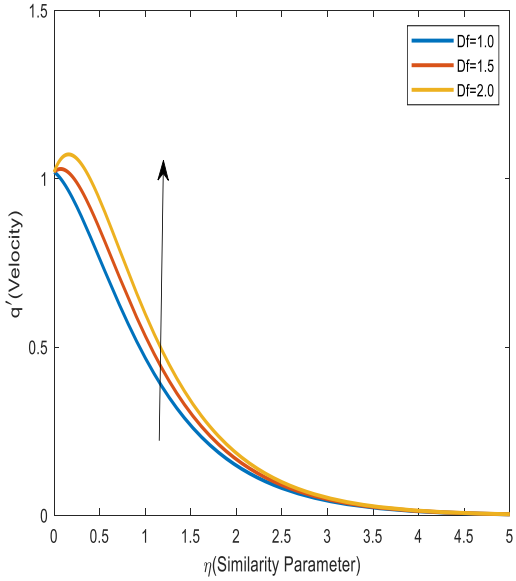


**Fig. 9.** Velocity Profile for different values of Df

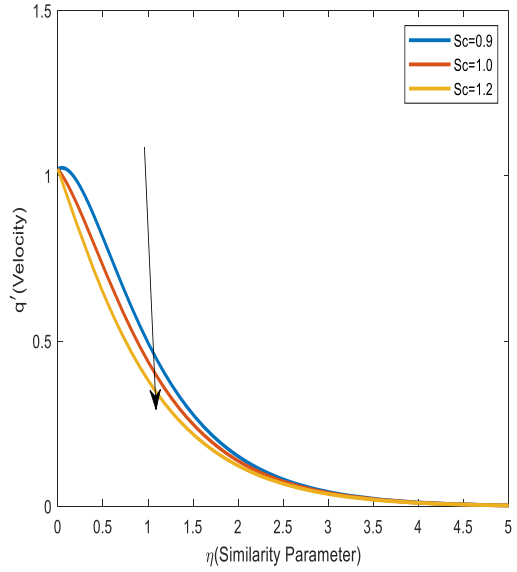


**Fig. 10.** Velocity Profile for different values of Sc

Fig.9 illustrates speed for thermal diffusion values it is evident that the highest speed is achieved if Dufour number gets high. In fig.10 displays plate's velocity contours at various Schmidt values. (Sc= 0.1, 0.3, 0.6). A plate's Schmidt number falls as speed rises.

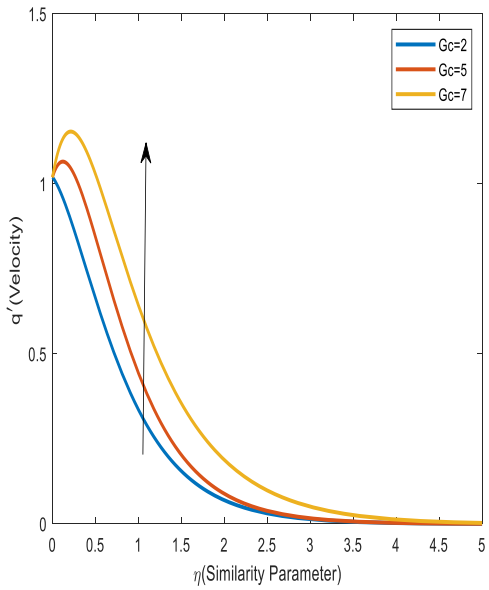


**Fig. 11.** Velocity Profile for different values of Gc

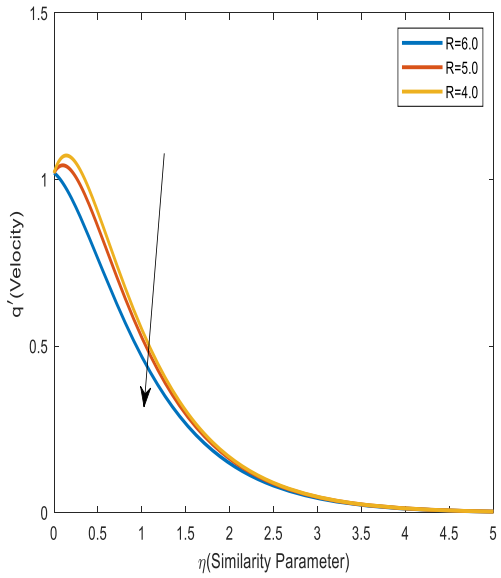


**Fig. 12.** Velocity Profile for different values of R

In fig.11 velocity contours of the plate are shown in the image above as increasing velocity causes the Gc values to increase. In fig.12 it is observed that velocity of the plate goes to down with an increasing the values of thermal radiation parameter R

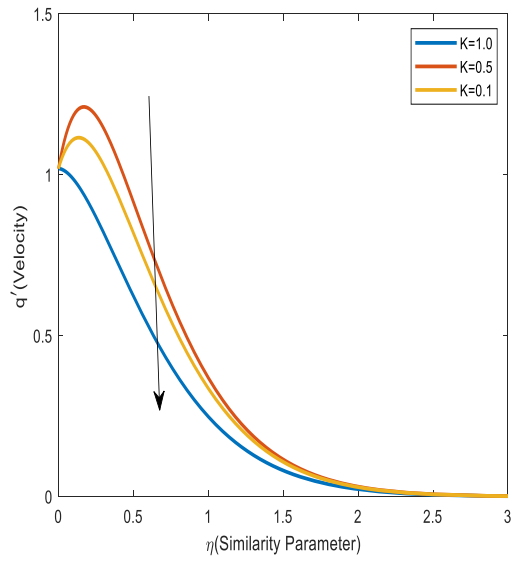


**Fig. 13.** Velocity Profile for different values of K

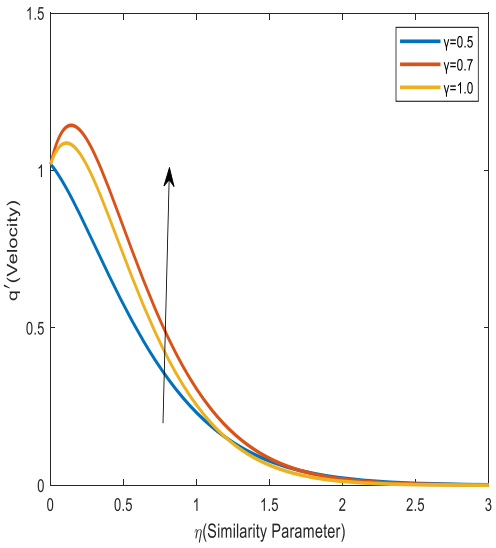


**Fig. 14.** Velocity Profile for different values of $\gamma$

In fig.13it is seen that velocity of the plate goes to down with an increasing the values of chemical reaction parameter K .In fig.14 it is seen that velocity of the plate goes to high performance with an increasing the values of Casson fluid parameter

## CONCLUSION

This research investigates the relationship between rotational effects and the Dufour effect. Specifically, we analyze the flow behavior of Casson fluid at constant temperature and concentration under the influence of thermal radiation and chemical reactions. By applying the Laplace transform, we gain deeper insights into the governing equations and interpret mathematical expressions to understand the fundamental flow characteristics.Graphs serve as an essential tool in this study, effectively visualizing data and highlighting variations in temperature, concentration, and velocity. The key findings are summarized as follows:

- **Temperature Profile:** The temperature increases with higher values of the Dufour number (Df), heat generation (Q), and time (t). However, it decreases with increasing Prandtl number (Pr), Schmidt number (Sc), chemical reaction parameter (K), and thermal radiation parameter (R)
- **Concentration Boundary Layer:** The concentration decreases over time (t) as the Schmidt number (Sc) and chemical reaction parameter (K) increase.
- **Velocity Profile:** The flow velocity decreases as the Dufour number (Df) increases. Additionally, an increase in the thermal gradient number (Gr), Casson fluid parameter (A), magnetic parameter (M), chemical reaction parameter (K), Schmidt number (Sc), thermal radiation parameter (R), and Prandtl number (Pr) further slows down the fluid motion.

## REFRENCES


[1] Soundalgekar, V. M., M. R. Patil, and M. D. Jahagirdar. "MHD Stokes problem for a vertical infinite plate with variable temperature." *Nuclear Engineering and design* 64, no. 1 (1981): 39-42. https://doi.org/10.1016/0029-5493(81)90030-3.

[2] Chamkha, Ali J., Harmindar S. Takhar, and V. M. Soundalgekar. "Radiation effects on free convection flow past a semi-infinite vertical plate with mass transfer." *Chemical Engineering Journal* 84, no. 3 (2001): 335-342.

[3] Kataria, Hari R., and Harshad R. Patel. "Radiation and chemical reaction effects on MHD Casson fluid flow past an oscillating vertical plate embedded in porous medium." *Alexandria Engineering Journal* 55, no. 1 (2016): 583-595. https://doi.org/10.1016/j.aej.2016.01.019.

[4] Vijayaragavan, R., M. Ramesh, and S. Karthikeyan. "Heat and Mass Transfer Investigation on MHD Casson Fluid Flow past an Inclined Porous Plate in the Effects of Dufour and Chemical Reaction." *Journal of Xi'an University of Architecture and Technology* 13 (2021): 860-873. http://dx.doi.org/10.37896/JXAT13.6/31183.

[5] Kavitha, S., Ayothi Selvaraj, Senthamilselvi Sathiamoorthy, and P. Rajesh. "A Parabolic Flow with MHD, the Dufour and Rotational Effects of Uniform Temperature and Mass Diffusion through an Accelerating Vertical Plate in the Presence of Chemical Reaction." Journal of Advanced Research in Fluid Mechanics and Thermal Sciences 110, no. 2 (2023): 192-205. https://doi.org/10.37934/arfmts.110.2.192205.

[6] Selvaraj, A., S. Dilip Jose, R. Muthucumaraswamy, and S. Karthikeyan. "MHD-parabolic flow past an accelerated isothermal vertical plate with heat and mass diffusion in the Presence of rotation." Materials Today: Proceedings 46 (2021): 3546-3549. https://doi.org/10.1016/j.matPr.2020.12.499

[7] Nandakumar, V., S. Senthamilselvi, and Ayothi Selvaraj. "Soret and MHD Effects of Parabolic Flow Past through an Accelerated Vertical Plate with Constant Heat and Mass Diffusion in the Presence of Rotation, Chemical Reaction and Thermal Radiation." *Journal of Advanced Research in Fluid Mechanics and Thermal Sciences* 112, no. 1 (2023): 125-138.https://doi.org/10.1016/j.matpr.2020.12.499.

[8] Selvaraj A., Jothi. 'Heat source impacts on MHD and radiation absorption fluid flow past an exponentially accelerated vertical plate with exponentially variable temperature and mass diffusion through porous medium.' Materials Today Proceeding 46, no.9: 3590-3594. https://doi.org/10.1016/j.matPr.2020.11.919

[9] Lakshmikaanth, D., A. Selvaraj, P. Selvaraju, and S. Dilip Jose. "Hall and heat source effects of flow past a parabolic accelerated isothermal vertical plate in the presence of chemical reaction and radiation." JP Journal of Heat and Mass Transfer 34 (2023): 105-126.https://doi.org/10.17654/0973576323035.

[10] Maran, D., A. Selvaraj, M. Usha, and S. Dilipjose. "First order chemical response impact of MHD flow past an infinite vertical plate with in the sight of exponentially with variable mass diffusion and thermal radiation." Materials Today: Proceedings 46 (2021): 3302-3307. https://doi.org/10.1016/j.matpr.2020.11.464

[11] Aruna, M., A. Selvaraj, and V. Rekha. "Hall and Magnetic Impacts on Stream Past a Parabolic Accelerated Vertical Plate with Varying Heat and Uniform Mass Diffusion in the Appearance of Thermal Radiation." In International Conference on Advancement in Manufacturing Engineering, pp. 323-336. Singapore: Springer Nature Singapore, 2022. https://doi.org/10.1007/978-981-99-1308-4_26.

[12] Radha, Ganesan, Ayothi Selvaraj, Soundararajan Bhavani, and Periasamy Selvaraju. "Magneto Hydrodynamic Effects on Unsteady Free Convection Casson Fluid Flow Past on Parabolic Accelerated Vertical Plate with Thermal Diffusion." Journal of Advanced Research in Fluid Mechanics and Thermal Sciences 116, no. 1 (2024): 184-200. https://doi.org/10.37934/arfmts.116.1.184200.

[13] Muthukumaraswamy, R., and P. Ganesan. "Unsteady flow past an impulsively started vertical plate with heat and mass transfer." Heat and Mass transfer 34, no. 2 (1998): 187-193.

[14] Muthucumaraswamy, R., M. Thamizhsudar, and J. Pandurangan. "Hall Effects On MHD Flow Past An Exponentially Accelerated Vertical Plate In The Presence Of Rotation." Annals of the Faculty of Engineering Hunedoara 12, no. 3 (2014): 145. https://doi:10.13140/RG.2.2.17206.14401

[15] Hetnarski, R. "On inverting the Laplace transforms connected with the error function." *Applicationes Mathematicae* 7, no. 4 (1964): 399-405.

[16] R.B.Hetnarski (1975): An algorithm for generating some inverse Laplace transform of exponential formZAMP Vol 26 , pp:249-253. https://doi.org/10.1007/bf01591514.

[17] Sarma, Subhrajit, and Nazibuddin Ahmed. "Dufour effect on unsteady MHD flow past a vertical plate embedded in porous medium with ramped temperature." Scientific Reports 12, no. 1 (2022): 13343.

[18] J Prakash A Selvaraj, "Effects of Radiation and Heat Generation on MHD and Parabolic Motion on Casson Fluids Flow Through a Rotating Porous Medium in a Vertical Plate", J. Appl. Math. & Informatics Vol. 42(2024), No. 3, pp. 607 – 623. https://doi.org/10.14317/jami.2024.607.

[19] Reddy, B. Prabhakar, O. D. Makinde, and Alfred Hugo. "A computational study on diffusion-thermo and rotation effects on heat generated mixed convection flow of MHD Casson fluid past an oscillating porous plate." International Communications in Heat and Mass Transfer 138 (2022): 106389. https://doi.org/10.1016/j.icheatmasstransfer.2022.106389.

[20] Reddy, N. Ananda, and K. Janardhan. "Soret and Dufour effects on MHD Casson fluid over a vertical plate in Presence of chemical reaction and radiation." Int. J. Curr. Res. Rev 9, no. 24 (2017): 55-61. DOI: 10.7324/IJCRR.2017.92411.

[21] Palani, G., and A. Arutchelvi A. Arutchelvi. "MHD Nanofluid Flow Past an Inclined Plate with Soret and Dufour Effects." Jp Journal of Heat and Mass Transfer 31 (2023): 123-145.https://doi.org/10.17654/0973576323009

[22] Kumar MA, Reddy YD. Combined effects of chemical reaction, Dufour, Soret effects on unsteady MHD flow past an impulsively started inclined porous plate with variable temperature and mass diffusion. Int. J. Math. Archive. 2016;7(9):98-111. https://doi.org/10.1016/j.ijft.2020.100061.

[23] Vempati SR, Laxmi-Narayana-Gari AB. Soret and Dufour effects on unsteady MHD flow past an infinite vertical porous plate with thermal radiation. Applied Mathematics and Mechanics. 2010 Dec;31:1481-96. https://doi.org/10.1007/s10483-010-1378-9

[24] Muthucumaraswamy R, Radhakrishnan M. Chemical reaction effects on flow past an accelerated vertical plate with variable temperature and mass diffusion in the Presence of magnetic field. Journal of Mechanical Engineering and Sciences. 2012 Dec 31;3:251-260.https://doi.org/10.15282/jmes.3.2012.1.0023

[25] Muthucumaraswamy R, Dhanasekar N, Prasad GE. Mass transfer effects on accelerated vertical plate in a rotating fluid with first order chemical reaction. Journal of Mechanical Engineering and Sciences. 2012 Dec 31;3:346-55https://doi.org/10.15282/jmes.3.2012.11.0033

[26] Patel, Harshad R. "Effects of cross diffusion and heat generation on mixed convective MHD flow of Casson fluid through porous medium with non-linear thermal radiation." Heliyon 5, no. 4 (2019). 1-26. **https://doi.org/10.1016/j.heliyon.2019.e01555**

[27] Dhanalakshmi, E., P. Rajesh, P. Kandan, M. Kesavan, G. Jayaraman, A. Selvaraj, and R. Priya. "Stability of bonds, kinetic stability, energy parameters, spectral characterization, GC–MS and molecular descriptors studies on coumarine, 3-[2-(1-methyl-2-imidazolylthio)-1-oxoethyl]." Journal of Molecular Structure 1295 (2024): 136544. https://doi.org/10.1016/j.molstruc.2023.136544.

[28] Karthikeyan, S., A. Selvaraj, and M. Venkateswarlu. "Rotating significance of parabolical movement antique with an appearance on isothermal vertical plate by MHD." *Materials Today: Proceedings* 51 (2022): 1120-1123. https://doi.org/10.1016/j.matpr.2021.07.098.

[29] Karthikeyan, S., and A. Selvaraj. "Uniform mass diffusion on thermal radiation with rotation of parabolic in progress vertical plate set MHD." *Materials Today: Proceedings* 51 (2022): 1074-1078. https://doi.org/10.1016/j.matpr.2021.07.109

[30] Gayathri, M., B. Hari Babu, and M. Veera Krishna. "Soret and Dofour effects on unsteady MHD convection flow over an infinite vertical porous plate." *Modern Physics Letters B* (2024): 2450449. https://doi.org/10.1142/S0217984924504499.

[31] Prakash, J., A. Selvaraj, P. Ragupathi, Qasem M. Al-Mdallal, and S. Saranya. "Thermal and Radiative Effects on Unsteady MHD Flow of Casson Fluid Past a Rotating Porous Medium with Variable Mass Diffusion." *Case Studies in Thermal Engineering* (2025): 105865.https://doi.org/10.1016/j.csite.2025.105865